PALEOECOLOGY

Global acceleration in rates of vegetation change over the past 18,000 years

Ondřej Mottl[1]*†, Suzette G. A. Flantua[1,2]*†, Kuber P. Bhatta[1], Vivian A. Felde[1,2], Thomas Giesecke[3], Simon Goring[4,5], Eric C. Grimm[6]‡, Simon Haberle[7,8], Henry Hooghiemstra[9], Sarah Ivory[10], Petr Kuneš[11], Steffen Wolters[12], Alistair W. R. Seddon[1,2], John W. Williams[4,5]

Global vegetation over the past 18,000 years has been transformed first by the climate changes that accompanied the last deglaciation and again by increasing human pressures; however, the magnitude and patterns of rates of vegetation change are poorly understood globally. Using a compilation of 1181 fossil pollen sequences and newly developed statistical methods, we detect a worldwide acceleration in the rates of vegetation compositional change beginning between 4.6 and 2.9 thousand years ago that is globally unprecedented over the past 18,000 years in both magnitude and extent. Late Holocene rates of change equal or exceed the deglacial rates for all continents, which suggests that the scale of human effects on terrestrial ecosystems exceeds even the climate-driven transformations of the last deglaciation. The acceleration of biodiversity change demonstrated in ecological datasets from the past century began millennia ago.

One of the clearest forms of biodiversity change during the past century has been the increased rates of species turnover across the marine and terrestrial biospheres (*1*–*3*). Today, >75% of Earth's ice-free land surface has been altered by human land use (*4*), with profound effects on the composition and functioning of ecosystems. Globally, extinction rates are increasing (*5*), although trends in local species richness are ambiguous (*6*).

These increased rates of species turnover, as signified by local and regional changes in community composition, are embedded in a longer-term context in which humanity's footprint has steadily grown since humans first began to alter landscapes for food, energy, and other resources. Hominid use of fire began at least 700,000 years ago (*7*), low-intensity but extensive agricultural land use began ~8000 years ago, and intensive agricultural land use expanded after 6000 years ago (*8*) (Fig. 1B). Detectable human imprints on vegetation began thousands of years ago (*9*, *10*), and the composition and carbon sequestration of many contemporary ecosystems remain profoundly influenced by the legacies of anthropogenic land use over the past centuries to millennia (*11*). Nonetheless, there remains a notable knowledge and scale gap between contemporary studies of global biodiversity trends of the past century (*2*) and studies examining early anthropogenic effects on ecosystems. Observational syntheses of global biodiversity trends are limited to the past several centuries, whereas macroscale syntheses of vegetation changes from fossil pollen data have been limited to continental scales (*9*) or are largely qualitative (*12*). Consequently, global patterns and magnitudes of vegetation compositional change, which are important for understanding how biodiversity and ecosystem dynamics have been shaped by climate change and early human activity, are poorly understood.

In parallel, paleoecological studies have shown the high sensitivity of terrestrial ecosystems to the climate changes that accompanied and followed the last deglaciation [~20,000 to 8200 calibrated years before radiocarbon present (cal yr BP, where 0 yr BP is 1950 CE); 20 to 8.2 thousand calibrated years BP (ka); Fig. 1, C and D] (*12*, *13*). In temperate and boreal regions, forest expanded from glacial refugia as temperatures rose and precipitation patterns shifted, with widespread leading-edge range expansions and, for some taxa, trailing-edge range contractions (*14*). Novel ecosystems emerged in response to novel climates and the Late Pleistocene extinction of megaherbivores (*15*). Tropical and subtropical ecosystems responded to rising temperatures linked to increasing greenhouse gases (Fig. 1D) and hydrological shifts driven by precessional controls on monsoons and the Intertropical Convergence Zone (*16*). Consequently, during the Pleistocene-Holocene transition, tropical ecosystems substantially changed in species composition and canopy structures across all elevations (*17*), whereas millennial- and centennial-scale hydroclimate variability caused abrupt changes in global vegetation during the Holocene (*18*).

Ecosystem responses to humans and climate change over long time scales can now be assessed globally, thanks to the century-long expansion of a global network of fossil pollen sequences anchored by increasingly precise radiocarbon chronologies (*19*); the building of open, community-curated data resources (*20*); and the development of new rate-of-change techniques (*21*). Here, we assess the global patterns and rates of vegetation change from the last deglaciation, through the Holocene, and up to the current Anthropocene on the basis of 1181 fossil pollen sequences from the Neotoma Paleoecology Database (*20*) covering all continents except Antarctica (Fig. 1 and data S1). These analyses are based on continentally harmonized taxonomies and updated Bayesian chronologies with age-depth model uncertainties and an improved algorithm [R package *R-Ratepol*; (*21*, *22*)] for estimating rates of change (RoCs) for paleoecological time series. RoCs are calculated as the compositional dissimilarity between consecutive time intervals (using the chi-squared coefficient) standardized by the length of time between samples, thereby providing an indicator of compositional change per unit of time. *R-Ratepol* uses a moving-window approach (instead of the traditional calculation of dissimilarities between individual levels), which minimizes artifactual alterations in RoC resulting from variations in sample density and sedimentation rate (*21*). *R-Ratepol* also incorporates temporal uncertainty resulting from age-depth modeling calculations through randomization (*21*, *22*). For each pollen sequence, we pooled data into 500-year time bins [see also our 250-year sensitivity experiment in the supplementary materials (*22*)] and calculated RoCs between bins to represent the rate of compositional change through time. For each sequence, we also identified time intervals with a large increase in RoC, called peak points [for more detailed information, see materials and methods (*22*)].

We analyzed RoCs at the scale of continents and subcontinental clusters, defined by climatic and geographic variables (*22*). For each continent and subcontinental region, we binned the RoC scores per 500-year time bins [with a 250-year sensitivity experiment in the supplementary materials (*22*)] and calculated the 95% RoC quantile to highlight intervals and places with large vegetation changes while filtering out outliers [see (*22*) for a comparison of the 95% quantile to median trends]. Similarly, we calculated the proportion of sequences with a peak point in each time bin. The clustering of peak points among sequences indicates a synchronous period of abrupt vegetation change within a region. Generalized additive models were fitted to all RoCs and peak point curves to

[1]Department of Biological Sciences, University of Bergen, N-5020 Bergen, Norway. [2]Bjerknes Centre for Climate Research, University of Bergen, N-5020 Bergen, Norway. [3]Department of Physical Geography, Utrecht University, 3508 TC, Utrecht, Netherlands. [4]Department of Geography, University of Wisconsin-Madison, Madison, WI, USA. [5]Center for Climatic Research, University of Wisconsin-Madison, Madison, WI, USA. [6]Department of Earth and Environmental Sciences, University of Minnesota, Minneapolis, MN, USA. [7]Department of Archaeology and Natural History, Australian National University, Canberra, ACT 2601, Australia. [8]Australian Research Council Centre of Excellence in Australian Biodiversity and Heritage, Australian National University, Canberra, ACT 2601, Australia. [9]Department of Ecosystem and Landscape Dynamics, University of Amsterdam, 1098 XH, Amsterdam, Netherlands. [10]Department of Geosciences and the Earth and Environmental Systems Institute (EESI), Penn State University, University Park, PA, USA. [11]Department of Botany, Faculty of Science, Charles University, Prague, Czech Republic. [12]Lower Saxony Institute for Historical Coastal Research, Wilhelmshaven, Germany.
***Corresponding author. Email: ondrej.mottl@gmail.com (O.M.); s.g.a.flantua@gmail.com (S.G.A.F.)**
†These authors contributed equally to this work.
‡Deceased.

summarize trends and test for significant accelerations [simultaneous confidence intervals of the first derivative differ from zero (*22*)].

We detect an unequivocal global acceleration of vegetation change during the Late Holocene (4.2 to 0 ka; Fig. 2). The estimated start of acceleration differs among continents and ranges from 4.6 to 3.1 ka (table S1). This estimated start is well supported by the dense availability of samples during the Middle to Late Holocene (Fig. 1E), but continental-scale estimates vary by ~500 to 1000 years (*22*). For most continents, Late Holocene RoCs are close to or exceed RoCs over the past 18 ka, with a percent differential ranging from −6.3 to 22.2% (Fig. 2 and table S1). Increases in RoC during the Lateglacial and Early Holocene can be linked to temperature and atmospheric CO_2 variations (Fig. 1, C and D) and hydrological variations. Rapid vegetation changes concentrate near the onset of the Holocene (11.7 ka) for most continents, expressed as a maximum in RoC or in peak points (Fig. 2). In North America and Europe, RoCs reached maxima during the abrupt millennial-scale climate oscillations characteristic of the North Atlantic and adjacent regions (~15 to 11 ka) and then substantially declined during the Early Holocene (Fig. 2, A and B). The heightened rates of deglacial vegetation change resemble the patterns of increased temperature variability in the North Atlantic and elsewhere in the Northern Hemisphere that were driven by a combination of orbital forcing, atmospheric greenhouse gas concentrations, meltwater pulses to the North Atlantic, and shifting patterns of heat transport (*23*). In Asia, rapid but asynchronous change characterizes the Lateglacial and deglaciation period, with a maximum in RoCs or a clustering

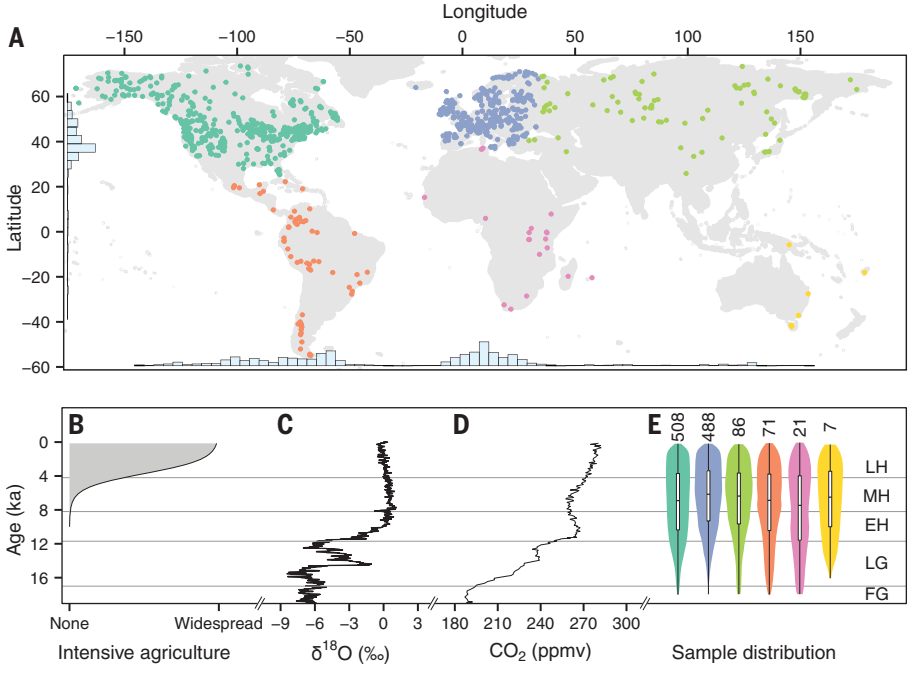

Fig. 1. Spatiotemporal distribution of the fossil pollen sequences analyzed here and climate and anthropogenic changes during the past 18,000 years. (**A**) Spatial distribution of pollen sequences used in this work. Histograms indicate the frequency of sequences across longitude and latitude. (**B**) Development of intensive agriculture based on archaeological expert elicitation (*8*). (**C**) $\delta^{18}O$, a temperature proxy, from the North Greenland Ice Core Project (NGRIP) (*38*). ‰, per mil. (**D**) Atmospheric CO_2 concentration [EPICA DOME C (*39*)]. ppmv, parts per million volume. (**E**) The number of pollen sequences per continent [colors match those in (A)] and sample density over the studied period. FG, full glacial; LG, Lateglacial; EH, Early Holocene; MH, Middle Holocene; LH, Late Holocene.

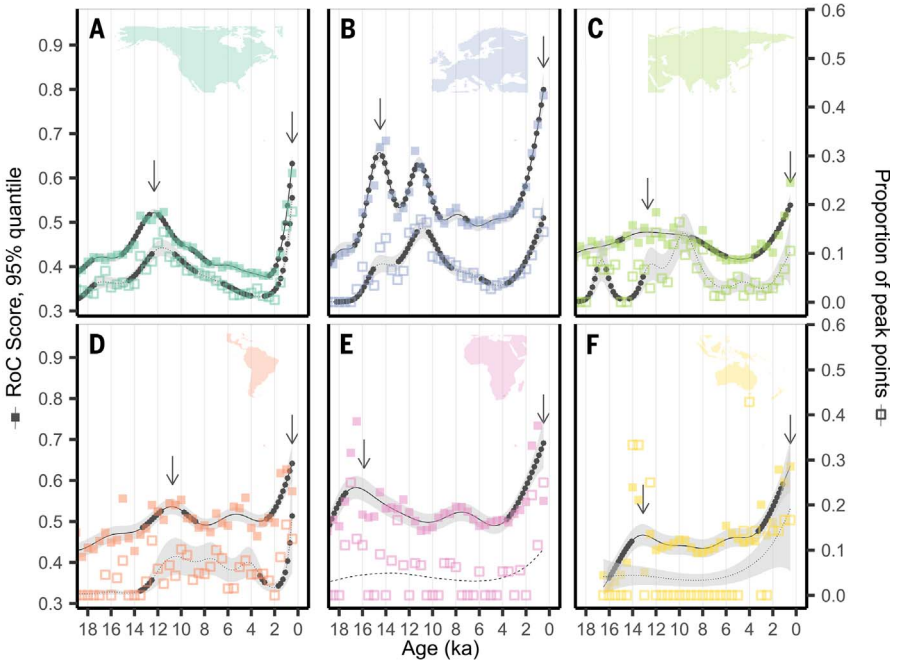

Fig. 2. RoC analyses by continent. (**A** to **F**) The filled squares represent the upper 95% quantile RoC score (left *y* axis) per 500-year time bin, with the solid curve representing the corresponding generalized additive model (GAM) (*22*). High values indicate high rates of vegetation change. Empty squares represent the proportion of peak points within each time bin (right *y* axis), with the corresponding GAM curve indicated by a dotted line. High values indicate a high synchrony in RoC among sequences (*22*). When the relationship is not significant, the GAM line is shown as dashed, and the error envelope is absent. Black asterisks on the GAM curves identify periods of significant acceleration in vegetation RoCs (i.e., where the derivative significantly differs from zero). Arrows indicate maximum RoC values for the Late Holocene and the Pleistocene-Holocene transition (table S1).

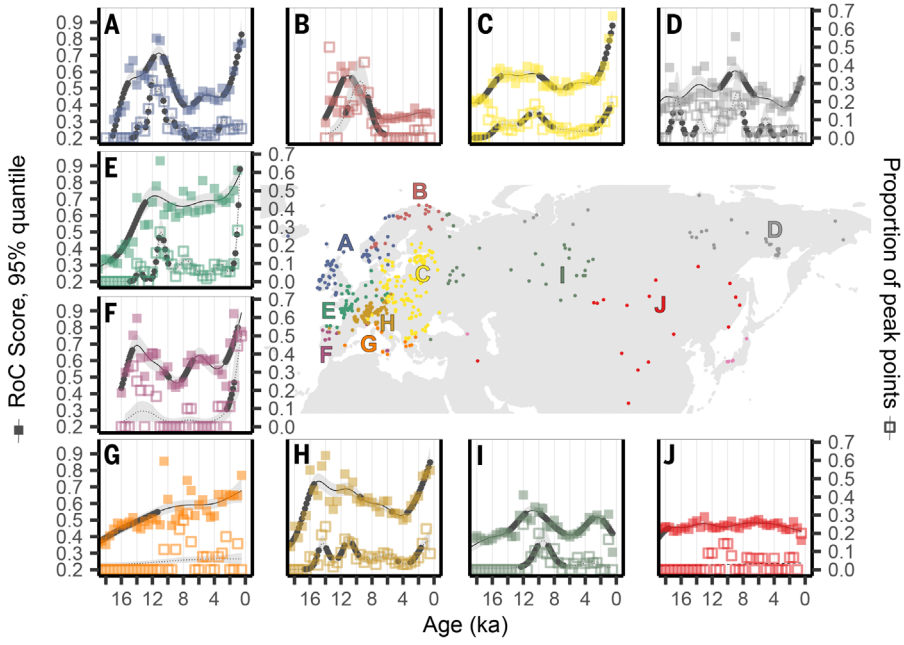

Fig. 3. RoC analyses by region across Eurasia. (**A** to **J**) Figure design follows that of Fig. 2.

of peak points between 10 and 8 ka (Fig. 2C). In Latin America and Africa, RoCs also reach maxima between 10 and 8 ka, which can be linked to altered monsoonal rainfall associated with declining Northern Hemisphere summer insolation (*24*).

RoC patterns at subcontinental scales are consistent with known histories of climate change and human land use. For example, in Eurasia, the western and northern European clusters show strong peaks in the rate of vegetation change between 15 and 10 ka (Fig. 3, A and E), which is consistent with the response of vegetation to North Atlantic climate variations and the retreating Eurasian ice sheets (Fig. 1C). Late Holocene rates of vegetation change are high across western and central Europe, particularly in areas of high present and past agricultural activity (*10*). In Asia, high rates of vegetation change during the Early Holocene can be linked to postglacial forest expansion in northern Asia (*25*) and millennial-scale variability in temperature and monsoonal rainfall in eastern Asia (*26*) (Fig. 3, C, D, and I). Seven of 10 Eurasian clusters show increased RoCs during the Late Holocene.

In the Americas, vegetation RoCs vary by latitude and between Atlantic- and Pacific-adjacent regions (Fig. 4). Eastern North America resembles western Europe in its high vegetation RoCs between 15 and 10 ka, with a strong signal of synchronous vegetation change over the past millennium (Fig. 4, G, H, and I). All North American regions show increased RoCs during the Late Holocene except for the high-latitude clusters. Driven by the topographic complexity of the Andes, vegetation responses in the Neotropical highlands were highly variable and asynchronous (Fig. 4D)—likely a combined effect of changes in temperature, hydroclimate variability, and atmospheric CO_2 (*27*, *28*). In the lowlands, a peak in vegetation RoCs at 10 ka is likely the result of hydrological variability linked to shifting monsoons (Fig. 4J) (*27*). These large vegetation changes challenge the common myth of the stable tropics and suggest a strong sensitivity of the Neotropics to temperature, hydroclimate variability, and orbital precession during the Early Holocene (*27*, *28*). In temperate South America, a period of synchronous vegetation change in the Holocene (Fig. 4E) is asynchronous with warm Neotropical regions (Fig. 4J), likely because of varying climate modes influencing different parts of the continent (*29*). The Late Holocene acceleration of vegetation change is clearly manifested across most of the latitudinal gradient of the Americas, except for the high northern latitudes, with the highest RoCs in coastal western North America and eastern North America (Fig. 4).

The detection of globally accelerating rates of vegetation change during the Late Holocene provides a longer-term perspective to the well-documented increase in species turnover during the 20th and 21st centuries (*6*). For terrestrial ecosystems at least, these recent increases in species turnover are the continuation of a longer acceleration that began millennia ago (Fig. 2). Moreover, this work suggests that contemporary communities and some current biodiversity trends may be partially resulting from legacies of past land use or environmental forcing (*11*) in combination with the strong anthropogenic imprint of the past decades. Hence, recent changes in biodiversity patterns represent only the most recent interval of our used planet (*30*) that has been altered by millennia of changing environments and human activities.

Our study focused primarily on detecting patterns of rates of vegetation compositional changes over the past 18,000 years and secondarily on attributing causes. This approach follows the standard delineation in climate change research between detection studies that focus on establishing the significance and fingerprints of observed climate trends (*31*) and attribution studies that explore the potential causes of the observed events and patterns (*32*). Biodiversity research is now achieving the capability for global detection analyses (*2*, *6*) across an increasingly broad range of time scales. The next frontier is to disentangle and attribute the contributions of climatic variability and anthropogenic impacts to past vegetation changes. This attribution is challenged by the complex interplay between climatic, anthropogenic, and vegetation dynamics that varies within and among ecosystems, particularly at local to regional scales. For example, in the Holocene in East Africa, land cover changes over the past 6000 years were driven by multiple cultural and technological innovations and by changes in rainfall amount and seasonality (*33*). In South America, Holocene climate variability contributed to regime shifts in human demography and displacement, which in turn affected ecosystems regionally (*34*). The worldwide spread of agricultural land use over the past 3000 years suggests intensified resource management (*8*) but was accompanied in some regions by substantial climate changes (*16*, *33*). Deglacial vegetation dynamics, although strongly climate driven, were also affected by global megaherbivore extinctions during the late Quaternary (*15*), which likely resulted from synergistic anthropogenic and climatic drivers (*35*). These interactions provide evidence against single-cause attributions of rates of vegetation change.

A key next step is to integrate these paleovegetation sequences with other paleoclimatic and archaeological records to better understand the past feedbacks among the climate, ecosystems, and humans (*3*, *10*, *13*, *36*) and the legacy effects of these past interactions on the trajectory of contemporary ecosystems. Assembled networks of paleovegetation, paleoclimatic, and anthropogenic records need to be harmonized and quality checked to do this attribution correctly and handle the spatial variations in vegetation, climate, and human histories within and among continents (*36*). Such an integration will also need carefully chosen numerical techniques to formally detect the onset of detectable human influence in paleoenvironmental time series and the variation in timing within and among ecosystems (*29*). Additionally, a higher density of paleoecological records is still needed, especially in topographically rich regions such as

Erratum 9 July 2021. See Erratum.

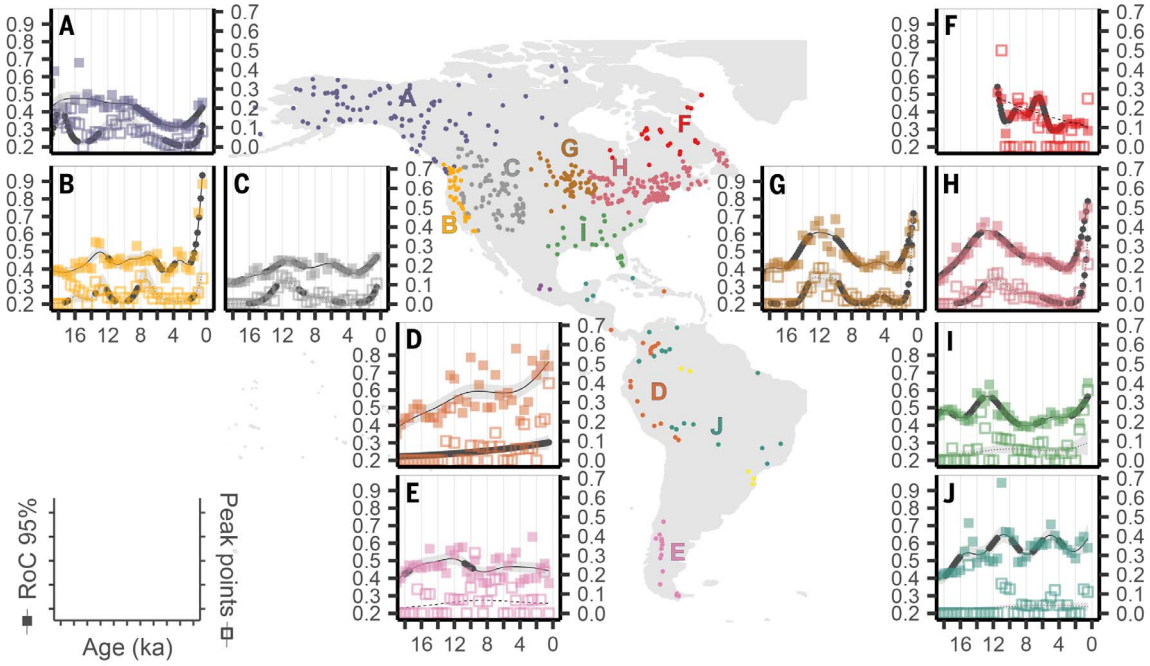

Fig. 4. RoC analyses by region across the Americas. (**A** to **J**) Figure design follows that of Fig. 2.

the Himalayas and the Andes, where climate heterogeneity is highest and human activities span millennia.

Despite these complexities, it is well known that the mean global temperature increases during the last deglaciation (~6°C) were several times as large as those of the Middle to Late Holocene [~1°C (*37*)]. Thus, a reasonable working inference is that the globally enhanced rates of vegetation change over the past several thousand years were caused primarily by anthropogenic activities, whereas vegetation changes during the Late Pleistocene to Early Holocene were driven primarily by changing climates. If so, the magnitude and extent of Late Holocene rates of vegetation change suggests that the global transformation of the terrestrial biosphere by humans now resembles or exceeds in rate and scope even the profound ecosystem transitions associated with the end of the last glacial period. Moreover, the global ecosystem changes for this century may be greater yet given current climate commitments and given that the climate changes expected for higher-end emission scenarios are similar in magnitude to those of the last deglaciation.

REFERENCES AND NOTES

1. B. J. McGill, M. Dornelas, N. J. Gotelli, A. E. Magurran, *Trends Ecol. Evol.* **30**, 104–113 (2015).
2. M. Dornelas *et al.*, *Glob. Ecol. Biogeogr.* **27**, 760–786 (2018).
3. J. Woodbridge *et al.*, *J. Ecol.* **109**, 1396–1410 (2021).
4. E. C. Ellis, N. Ramankutty, *Front. Ecol. Environ.* **6**, 439–447 (2008).
5. S. L. Pimm *et al.*, *Science* **344**, 1246752 (2014).
6. S. A. Blowes *et al.*, *Science* **366**, 339–345 (2019).
7. D. M. J. S. Bowman *et al.*, *J. Biogeogr.* **38**, 2223–2236 (2011).
8. L. Stephens *et al.*, *Science* **365**, 897–902 (2019).
9. T. Giesecke *et al.*, *Nat. Commun.* **10**, 5422 (2019).
10. L. Marquer *et al.*, *Quat. Sci. Rev.* **171**, 20–37 (2017).
11. C. N. H. McMichael, *New Phytol.* **229**, 2492–2496 (2021).
12. C. Nolan *et al.*, *Science* **361**, 920–923 (2018).
13. D. A. Fordham *et al.*, *Science* **369**, eabc5654 (2020).
14. J. W. Williams, B. N. Shuman, T. Webb III, P. J. Bartlein, P. L. Leduc, *Ecol. Monogr.* **74**, 309–334 (2004).
15. Y. Malhi *et al.*, *Proc. Natl. Acad. Sci. U.S.A.* **113**, 838–846 (2016).
16. F. E. Mayle, D. J. Beerling, W. D. Gosling, M. B. Bush, *Phil. Trans. R. Soc. Lond. B* **359**, 499–514 (2004).
17. F. E. Mayle, M. J. Burn, M. Power, D. H. Urrego, in *Past Climate Variability in South America and Surrounding Regions*, F. Vimeux, F. Sylvestre, M. Khodri, Eds., vol. 14 of *Developments in Paleoenvironmental Research* (Springer, 2009), pp. 89–112.
18. A. W. Seddon, M. Macias-Fauria, K. J. Willis, *Holocene* **25**, 25–36 (2015).
19. S. G. A. Flantua *et al.*, *Rev. Palaeobot. Palynol.* **223**, 104–115 (2015).
20. J. W. Williams *et al.*, *Quat. Res.* **89**, 156–177 (2018).
21. O. Mottl *et al.*, bioRxiv 2020.12.16.422943 [Preprint]. 24 February 2021. https://doi.org/10.1101/2020.12.16.422943.
22. See supplementary materials online.
23. Z. Liu *et al.*, *Science* **325**, 310–314 (2009).
24. T. M. Shanahan *et al.*, *Nat. Geosci.* **8**, 140–144 (2015).
25. G. M. MacDonald, K. V. Kremenetski, D. W. Beilman, *Phil. Trans. R. Soc. B* **363**, 2283–2299 (2008).
26. H. Zhang *et al.*, *Quaternary* **2**, 26 (2019).
27. V. F. Novello *et al.*, *Earth Planet. Sci. Lett.* **524**, 115717 (2019).
28. M. H. M. Groot *et al.*, *Clim. Past* **7**, 299–316 (2011).
29. S. G. A. Flantua *et al.*, *Clim. Past* **12**, 483–523 (2016).
30. E. C. Ellis *et al.*, *Proc. Natl. Acad. Sci. U.S.A.* **110**, 7978–7985 (2013).
31. PAGES 2k Consortium, *Nat. Geosci.* **6**, 339–346 (2013).
32. K. E. Trenberth, J. T. Fasullo, T. G. Shepherd, *Nat. Clim. Chang.* **5**, 725–730 (2015).
33. R. Marchant *et al.*, *Earth Sci. Rev.* **178**, 322–378 (2018).
34. P. Riris, M. Arroyo-Kalin, *Sci. Rep.* **9**, 6850 (2019).
35. E. D. Lorenzen *et al.*, *Nature* **479**, 359–364 (2011).
36. A. Bevan *et al.*, *Proc. Natl. Acad. Sci. U.S.A.* **114**, E10524–E10531 (2017).
37. J. E. Tierney *et al.*, *Nature* **584**, 569–573 (2020).
38. North Greenland Ice Core Project members, *Nature* **431**, 147–151 (2004).
39. E. Monnin *et al.*, *Science* **291**, 112–114 (2001).
40. O. Mottl, S. Flantua, HOPE-UIB-BIO/Global_RoC, version v1.1, Zenodo (2021); http://doi.org/10.5281/zenodo.4972077.
41. S. G. A. Flantua *et al.*, "Mottl et al. (2021, Science) Taxonomic harmonization tables for North America, Latin America, Europe, Asia, Africa," Figshare, dataset (2021); https://doi.org/10.6084/m9.figshare.13049735.

ACKNOWLEDGMENTS

We are grateful to all data contributors to the Neotoma Paleoecology Database and data stewards for the constituent databases—African Pollen Database, European Pollen Database, IndoPacific Palaeoecology Database, Latin American Pollen Database, and North American Pollen Database—for supporting open-access data. We thank H. J. B. Birks for making suggestions on the analyses and for providing advice on the Asian taxonomic harmonization. **Funding:** O.M., S.G.A.F., K.P.B., V.A.F., and A.W.R.S. acknowledge support from the European Research Council (ERC) under the European Union's Horizon 2020 research and innovation program (grant agreement no. 741413) to H. J. B. Birks. Neotoma development has been supported by the National Science Foundation (1550707, 1550805, and 1948926) and Belmont Forum (1929476). **Author contributions:** O.M., S.G.A.F., A.W.R.S., and J.W.W. co-led and designed the study. S.G.A.F., K.P.B., V.A.F., A.W.R.S., and O.M. developed the data extraction workflow, and O.M. performed the numerical analyses. J.W.W., H.H., S.G.A.F., K.P.B., and S.I. led the compilation and taxonomic harmonization of continental-scale pollen datasets. E.C.G., T.G., S.H., H.H., S.I., S.G.A.F., and J.W.W. led Neotoma data mobilization efforts. S.G.A.F. and J.W.W. led the writing. All authors contributed to the article and approved the submitted version. **Competing interests:** The authors declare no competing interests. **Data and materials availability:** All the data and R codes are publicly available at Zenodo (*40*) and at https://github.com/HOPE-UIB-BIO/Global_RoC. Harmonization tables are available at Figshare (*41*).

SUPPLEMENTARY MATERIALS

science.sciencemag.org/content/372/6544/860/suppl/DC1
Materials and Methods
Figs. S1 to S7
Tables S1 to S3
References (*42*–*77*)
Data S1

19 December 2020; accepted 8 April 2021
10.1126/science.abg1685